JOURNAL OF THERMOPHYSICS AND HEAT TRANSFER
Vol. 22, No. 4, October–December 2008

Modeling of Processing for Slot and Discrete Port Tapered Resin Injection Pultrusion

A. L. Jeswani* and J. A. Roux†
University of Mississippi, University, Mississippi 38677

DOI: 10.2514/1.33209

Pultrusion is a very cost-effective method for manufacturing structural components of constant cross sections for aerospace applications and for a broad range of other engineering applications. The quality and mechanical strength of the pultruded part depends on the wet out of the fiber reinforcement by the liquid resin; the strength and, thus, the quality of the composite are superior when the fiber reinforcement is fully impregnated (complete wet out) with liquid resin. This work explores the wet-out characteristics in the injection pultrusion process. Complete wet out of the dry fiber matrix with liquid resin depends significantly on the processing parameters. The process parameters, fiber pull speed, fiber volume fraction, and resin viscosity are explored in this study. The finite volume technique is employed to simulate the flow of polyester resin through the fiber matrix (glass rovings), and the impact of the process parameters on the injection pressure required to achieve complete fiber wet out is investigated. The location of the liquid resin flow front is predicted for the discrete port injection and the slot injection configurations. The results show the impact of the tapering of the injection chamber walls on the minimum injection pressure required to achieve complete fiber wet out and the corresponding resin pressure at the injection chamber exit. A small taper on the walls of the injection chamber was found to have a significant impact on the minimum injection pressure necessary to achieve complete fiber matrix wet out.

Introduction

PULTRUSION is a very important manufacturing process for producing structural components for a wide variety of aerospace vehicles. Thus, improving pultrusion manufacturing has a direct impact on the aerospace industry's efficiency and competitiveness. Pultrusion machines consist of the following: a creel, a resin wet-out chamber, forming dies, a heated die, pullers, and a cutoff saw. A schematic of resin injection pultrusion (closed bath technique) is given in Fig. 1. The fiber reinforcement is pulled through the injection chamber and resin is injected into the fiber matrix under pressure. As the resin is injected under pressure, good wet out of the fiber reinforcement must be achieved. Next, the fiber/resin system is passed through the heated die, where curing of the fiber matrix and resin occurs. Injection pultrusion produces significantly lower volatile emissions as compared with open bath wet-out methods. Also, resins with low pot life can be used with the injection pultrusion process; throughput of a resin injection system is high and desirable for high productivity.

Experimental research has been conducted at the University of Mississippi [1], the University of Minnesota [2], and the University of Massachusetts at Lowell [3] to investigate the injection pultrusion process. Numerical models for the injection pultrusion process are generally built on similar numerical schemes that were developed for the flow simulation of the resin transfer molding process [4–7]. Liu [8] developed a finite element/nodal volume technique to model the resin flow through the matrix during the injection pultrusion process. Liu [9] also developed transient and iterative finite element/nodal volume models to predict the steady-state flow front. Only one injection slot, located on top of the injection chamber, was used for injecting resin through the fiber reinforcement. This model was used to simulate the liquid resin flow at very low pull speeds. The impact of different processing parameters was not presented in this work.

Ding et al. [10] at Ohio State University have developed a 2-D control volume/finite element model for flow simulation of injection pultrusion. The model was applied to generate a process window for the injection pultrusion of fiberglass–vinyl ester composites [11]. This work did not consider material property (viscosity, fiber volume fraction) variations. Rahatekar and Roux [12] developed a 2-D finite volume method to predict the resin pressure field, resin velocity field, and resin moving flow front location. A numerical model for flow simulation and the curing of resin was developed by Kommu et al. [13] using the finite element/control volume and finite difference techniques; the simulation results were presented at very low pull speeds. The impact of the variation of other processing parameters such as fiber volume fraction and resin viscosity was not presented in their work. Voorakaranam et al. [14] developed a 2-D model to simulate resin flow, cure, and heat transfer. The injection pultrusion process was studied from the point of view of product quality control to maximize production rates. Raper et al. [15] presented a 2-D model for the open bath method of achieving fiber matrix wet out using the finite volume approach, but resin injection (closed bath) is needed for the high pull speeds and fast curing resin systems required for high productivity.

This work corresponds to the pultrusion manufacturing of a polyester resin/glass roving composite, which requires significantly higher pull speeds for high product yield. To check the validity of results from the current numerical model, the simulations were performed with the parameters reported in Liu [8,9] and Rahatekar and Roux [12], and excellent agreement was observed with the results reported in those references.

Statement of the Problem

Wet out is essential for the pultrusion manufacturing of composites. Complete wet out of the fiber matrix helps to manufacture a good quality product with good mechanical properties. If the pull speed is high, then complete wet out is difficult to attain and high injection pressures must be employed to achieve complete wet out. Composites with high fiber volume fractions require high injection pressures to achieve wet out because the resin flow is restricted by the higher number of fibers. Similarly, higher viscosity resins offer higher resistance to flow through the fiber

Presented as Paper 4104 at the 37th AIAA Fluid Dynamics Conference and Exhibit, Miami, FL, 25–28 June 2007; received 2 July 2007; revision received 2 March 2008; accepted for publication 2 March 2008.

*Graduate Student, Department of Mechanical Engineering. Member AIAA.

†Faculty, Department of Mechanical Engineering. Associate Fellow AIAA.

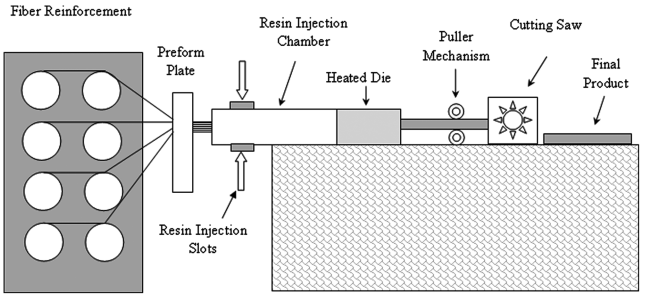

Fig. 1 Schematic of resin injection pultrusion.

reinforcement and, thus, require higher injection pressures. The aforementioned process parameters (fiber pull speed, fiber volume fraction, and resin viscosity) are interdependent; thus, an understanding of the individual and coupled effects of these parameters is desired. These can be investigated with the present 3-D numerical model; this model can be useful in guiding improvements for achieving complete wet out in the resin injection chamber. In this work, the resin injection chamber (where wet out of fiber matrix is achieved) is attached to the pultrusion die and is located upstream of the die heating zone but thermally insulated from the heated die. Thus, the resin flow is modeled as isothermal. Curing inside the injection chamber would be a poor injection chamber design and undesirable; the purpose of the injection chamber is to achieve complete wet out before curing starts. Figures 2 and 3 depict the different geometric regions of the injection chamber for the discrete port injection and slot injection, respectively. The computational domain (injection chamber) is divided into two regions (regions 1 and 2). Region 1 is where the injection slots/ports are located; region 2 is the latter part of the injection chamber, which is also the entrance part of the pultrusion die. L_{ic} and L_D are the lengths of regions 1 (injection chamber) and 2 (die entrance) and are taken to be 0.25 and 0.05 m, respectively.

For the slot injection configuration (Fig. 2), a 0.01-m wide injection slot is placed at $x = 0.10$ m from the front boundary and is located on both the top and bottom walls of the injection chamber. For the discrete port injection configuration (Fig. 3), five discrete

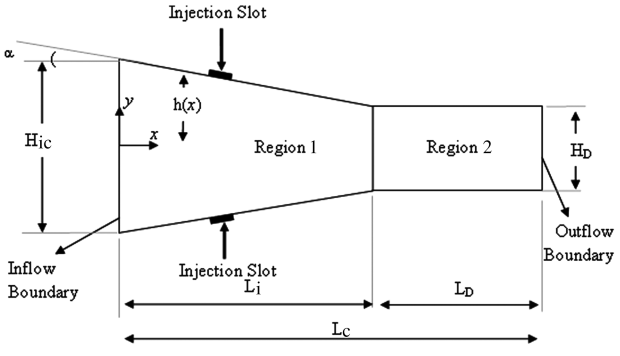

a) In *xy* plane (front view)

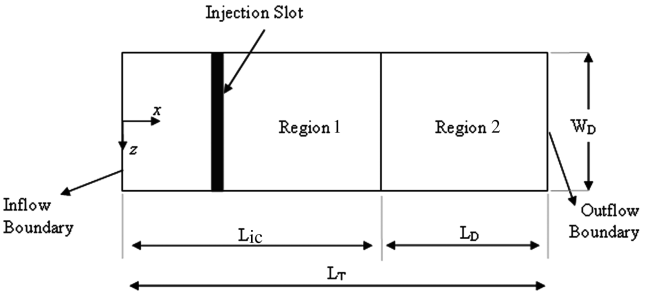

b) In *xz* plane (top view)

Fig. 2 Schematic of the computational domain for the slot injection chamber configuration (not to scale).

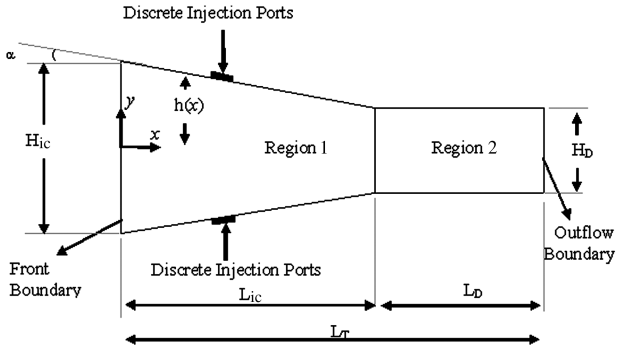

a) In *xy* plane (front view)

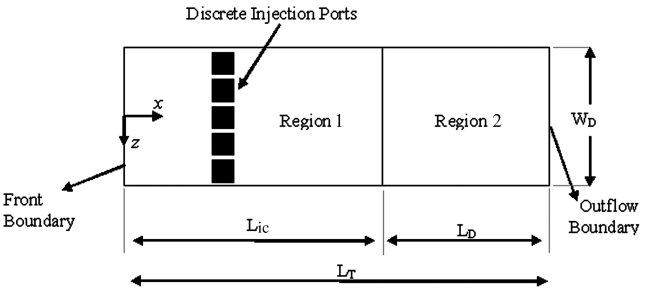

b) In *xz* plane (top view)

Fig. 3 Schematic of the computational domain for the discrete port injection chamber configuration (not to scale).

ports, each 0.01×0.01 m^2 with a gap of 5 mm between adjacent ports and a gap of 2.5 mm between the port and the die side walls, were employed to study the impact of the processing parameters. H_{ic} and W_D correspond to the height and width of the front boundary region 1, and H_D and W_D are the height and width of the exit portion of region 2 (thickness and width of final composite part). The compression ratio is defined as $CR = H_{ic}/H_D$. The injection chamber is considered to be attached to the pultrusion die. A pump injects the resin under pressure through the injection slots/ports. Dry fiber reinforcement enters the injection chamber and, as it passes through region 1, the liquid resin wets the fibers. Region 2 has a constant cross section, and so the fiber volume fraction and permeability are constant in this region but are functions of the axial distance (x) in region 1. At the exit of the computational domain, it was considered that the fiber reinforcement and the resin are moving at the same velocity as in Liu [8,9], Rahatekar and Roux [12], and Raper et al. [15].

The finite volume method [16] is employed to compute the pressure field, the flowfield, and the liquid resin flow front location. The number of mesh points in the x, y, and z directions was 242, 20, and 14, respectively, for the injection slot configuration and 242, 20, and 34 nodes for the discrete port configuration. The CPU run time (Dell Optiplex, 3.8 GHz, 2 GB RAM) was from less than 1 min to less than 6 h depending on the case study. The program produced excellent agreement when verified with the results reported in Liu [9] and Rahatekar and Roux [12].

Analysis

Governing Equations for Regions 1 and 2 of the Injection Chamber

The model used for the flow of resin within the saturated fiber reinforcement is based on Darcy's law [17]. The continuity equation for the flow of resin within the saturated reinforcement is expressed by

$$\frac{\partial(u\phi)}{\partial x} + \frac{\partial(v\phi)}{\partial y} + \frac{\partial(w\phi)}{\partial z} = 0 \tag{1}$$

where, in region 1, u, v, and w are the components of resin velocity in the three coordinate directions and are defined as follows:

$$u = U - \frac{K_{11}}{\mu\phi}\frac{\partial P}{\partial x}, \qquad v = V - \frac{K_{22}}{\mu\phi}\frac{\partial P}{\partial y}, \qquad w = -\frac{K_{33}}{\mu\phi}\frac{\partial P}{\partial z} \quad (2)$$

where P is the resin pressure, ϕ is the porosity, and U and V are the velocity components of the fiber reinforcement in the x, and y directions, respectively. $-\frac{K_{11}}{\mu\phi}\frac{\partial P}{\partial x}$, $-\frac{K_{22}}{\mu\phi}\frac{\partial P}{\partial y}$, and $-\frac{K_{33}}{\mu\phi}\frac{\partial P}{\partial z}$ are the three components of the liquid resin velocity relative to the reinforcement. K_{11} (x direction), K_{22} (y direction), and K_{33} (z direction) are the components of the permeability tensor and μ is the viscosity of the resin. Equation (3) expresses the relation between the fiber velocity in the y direction (V) in terms of the taper angle (α), the fiber velocity in the x direction (U), and the position in the y direction as

$$V = -U(y/h(x))\tan\alpha \quad (3)$$

where the distance y (see Figs. 2 and 3) varies as $-h(x) \leq y \leq h(x)$ and $h(x) = m_1 x + b_1$, and where $m_1 = \tan\alpha$. Substituting Eqs. (2) and (3) into Eq. (1) yields the following pressure equation:

$$\frac{\partial}{\partial x}\left(\frac{K_{11}}{\mu}\frac{\partial P}{\partial x}\right) + \frac{\partial}{\partial y}\left(\frac{K_{22}}{\mu}\frac{\partial P}{\partial y}\right) + \frac{\partial}{\partial z}\left(\frac{K_{33}}{\mu}\frac{\partial P}{\partial z}\right) = U\left\{\frac{\partial \phi}{\partial x} - \frac{\phi}{h(x)}\tan\alpha\right\} \quad (4)$$

Equation (4) is the governing pressure equation for region 1. Because of the tapered wall of the injection chamber in region 1, the right-hand side of Eq. (4) acts like a source for pressure and, hence, produces a pressure rise in liquid resin. In region 2 of the injection chamber, the walls are not tapered ($\alpha = 0$) and so the fiber velocity in the transverse directions ($V = 0$) is equal to zero. Because U and ϕ are constant in region 2, the term $\frac{\partial \phi}{\partial x}$ vanishes and Eq. (4) simplifies to

$$\frac{\partial}{\partial x}\left(\frac{K_{11}}{\mu}\frac{\partial P}{\partial x}\right) + \frac{\partial}{\partial y}\left(\frac{K_{22}}{\mu}\frac{\partial P}{\partial y}\right) + \frac{\partial}{\partial z}\left(\frac{K_{33}}{\mu}\frac{\partial P}{\partial z}\right) = 0 \quad (5)$$

Equation (5) is the governing pressure partial differential equation for region 2 of the injection chamber.

Fiber Volume Fraction and Porosity

The fiber volume fraction (V_{fo}) is defined as the volume fraction of fiber in the final composite; whereas V_f corresponds to the local fiber volume, ($V_f = V_f(x)$). The fraction of nonsolid volume is termed as porosity, ϕ. The porosity, ϕ, and the fiber volume fraction, V_f, can be functions of distance (x) in the longitudinal direction. In region 1 of the computational domain, the walls of the injection chamber are tapered so that the fiber volume fraction (V_f), porosity (ϕ), and components of the permeability (K_{11}, K_{22}, and K_{33}) are functions of axial distance (x). In region 2 of the computational domain, the fiber volume fraction and the porosity do not vary with the x location because the cross-sectional area remains constant; hence, $V_f(x)$ and $\phi(x)$ are constants (here $V_f(x) = V_{fo}$). The local porosity $\phi(x)$ and local fiber volume fraction $V_f(x)$ are related by $\phi(x) = 1 - V_f(x)$. In region 1, the local fiber volume fraction, $V_f(x)$, is given by

$$V_f(x) = V_{fo}(H_D/2h(x)) \quad (6a)$$

where

$$h(x) = -\left(\frac{H_{ic} - H_D}{2L_{ic}}\right)(x - L_{ic}) + (H_D/2) \quad (6b)$$

Boundary Conditions

The computational domain is symmetric about the xy and xz planes. By taking advantage of this symmetry, only a quarter of the computational domain needs to be modeled. The pressure boundary conditions corresponding to Eqs. (4) and (5) are given as follows:

$$P = P_{atm} \quad \text{at } x = 0 \quad (7a)$$

$$P = P_{inj} \text{ at injection port/slot} \quad (7b)$$

$$\frac{K_{11}}{\mu\phi}\frac{\partial P}{\partial x}\sin\alpha + \frac{K_{22}}{\mu\phi}\frac{\partial P}{\partial y}\cos\alpha = 0 \quad \text{at } y = h(x) \text{ (region 1)} \quad (7c)$$

$$\frac{\partial P}{\partial y} = 0 \quad \text{at } y = 0 \text{ (region 1)} \quad (7d)$$

$$\frac{\partial P}{\partial z} = 0 \quad \text{at } z = W_D/2 \text{ (region 1)} \quad (7e)$$

$$\frac{\partial P}{\partial z} = 0 \quad \text{at } z = 0 \text{ (region 1)} \quad (7f)$$

$$\frac{\partial P}{\partial y} = 0 \quad \text{at } y = H_D/2 \text{ (region 2)} \quad (7g)$$

$$\frac{\partial P}{\partial y} = 0 \quad \text{at } y = 0 \text{ (region 2)} \quad (7h)$$

$$\frac{\partial P}{\partial z} = 0 \quad \text{at } z = W_D/2 \text{ (region 2)} \quad (7i)$$

$$\frac{\partial P}{\partial z} = 0 \quad \text{at } z = 0 \text{ (region 2)} \quad (7j)$$

$$\frac{\partial P}{\partial x} = 0 \quad \text{at } x = L_T \text{ (length of injection chamber)} \quad (7k)$$

In regions 1 and 2, because a slip boundary condition is used along the wall, Eqs. (7c–7j) are the pressure boundary conditions; these are obtained by setting the component of the resin velocity normal to the injection chamber wall equal to zero (no penetration of resin into the wall). It is taken as in [12,15,18] that, at the outlet of the injection chamber, the resin velocity in the x direction is equal to the fiber velocity in the x direction ($u = U$). Darcy's law [Eq. (2)] [17] of flow through a porous medium is used to simulate resin flow through a fiber matrix. The resistance of the reinforcement fiber to resin flow is characterized by the permeability, and the following two models predict the components of the permeability tensor: Kozeny–Carman [19] model (K_{11}) and Gutowski's [19] model ($K_{22} = K_{33}$). The hexagonal fiber arrangement, effective fiber diameter of 30 μ, and the permeability constants from Gutowski's [19] work were employed. The compression ratio ($CR = H_{ic}/H_D$) determines the degree of tapering of the injection chamber walls.

Algorithm for Time Marching Scheme

To solve the governing pressure partial differential equation [Eqs. (4) and (5)], the line-by-line tri-diagonal matrix algorithm technique [16] was employed to determine the pressure field of resin for the entire computational domain. The overall solution marches forward by a time marching procedure. Having solved the pressure field at each time step, the velocity field is obtained by the finite differencing of Darcy's equations [Eqs. (2)]. The net liquid resin mass flow rate is calculated for all the control volumes in the domain. Each control volume in the domain is assigned a resin fill factor. The fill factor, $F_{i,j,k}$, is the fraction of the control volume occupied by the

liquid resin at a given time instant relative to the maximum liquid resin the control volume can hold. In the numerical scheme, $F_{i,j,k}$ is related to the amount of resin in a given control volume. For a completely liquid filled control volume, the value of $F_{i,j,k}$ is unity (saturated reinforcement) and is zero (dry reinforcement) if the control volume is empty of liquid. The pressure is computed at a control volume if it is fully saturated with liquid resin; otherwise, atmospheric pressure is assigned to it. Then the time needed to fill the as yet unfilled control volumes was determined. The minimum value of the time step is the amount of time required to fill the next quickest-to-fill control volume, which has resin in it but is not yet completely filled, and yet not overfill any other control volume. As the flow front is advanced through time using this minimum time step, it is ensured that, at most, only one control volume is filled in one time step and no control volume is overfilled as time advances forward. The fill factors of all unfilled or not completely filled control volumes (where $0 \leq F_{i,j,k} < 1$) are updated at the end of each time step by using the minimum time step. To maintain the numerical stability of the algorithm, the pultruded part is not allowed to travel by more than the length of the nodal control volume in the pull direction during a given time step, that is,

$$0 < \Delta t_{\min} < (L_{\min}/U) \tag{8}$$

where $L_{\min}$ is minimum length of the control volume in the pull speed direction and U is the fiber pull speed in the longitudinal direction. This is a default time step size, and time is not allowed to advance by an amount greater than that given in Eq. (8). Hence, it is possible that no new control volumes are filled during a time step. This condition is checked at every time step and no more than one control volume is allowed to be newly filled at that time step. The criterion used to determine the steady state is when both the liquid resin flow front and the resin pressure field do not change in time; this typically occurs in less than 20 s of simulated time. When the steady state is reached, no new control volumes are filled and the liquid resin flow front does not move as time progresses.

Results and Discussion

In this study, the impact of the tapering of the injection chamber walls on the minimum injection pressure necessary to achieve complete wet out and the injection chamber exit resin pressure are demonstrated for various processing parameters (pull speed, fiber volume fraction, and resin viscosity) for the slot injection and the discrete port injection configurations. Each process parameter was varied while the other process parameters were held at their nominal values. The nominal parameter values selected for this study were as follows: pull speed, $U = 0.0254$ m/s (60 in./min); fiber volume fraction, $V_{fo} = 0.68$; and resin viscosity, $\mu = 0.75$ Pa · s. In the first part of this study, five discrete ports (see Fig. 2), each 0.01×0.01 m^2 with a gap of 5 mm between adjacent ports and a gap of 2.5 mm between the port and the die side walls, were used to study the impact of the processing parameters. In the second part, a 0.01-m wide injection slot located at $x = 0.1$ m from the inflow boundary (see Fig. 3) was employed. In this study, the results are presented for an injection chamber attached to the pultrusion die entrance. The typical values of the compression ratio ($CR = H_{ic}/H_D$) and the taper angle, α (degrees), investigated here were $CR = 1.0(\alpha = 0.00000)$, $1.2(\alpha = 0.07276)$, $1.5(\alpha = 0.18190)$, and $2.0(\alpha = 0.36380)$. The liquid resin pressures are expressed in gauge pressure. The final pultruded composite is 0.003175-m ($H_D = 0.125$ in.) thick and 0.0635-m ($W_D = 2.5$ in.) wide.

Discrete Port Injection Configuration

In this section, the results are presented for various processing parameters for the discrete port injection configuration. Table 1 summarizes the minimum injection pressures necessary for complete part wet out at different pull speeds (cases 1–3 and 8–11), fiber volume fractions (cases 3–5 and 10, 12–14), and different resin viscosities (cases 3, 6, 7, and 10, 15–17) at $CR = 1.0$ and 1.2; injection pressures below the values given in Table 1 result in incomplete fiber matrix wet out.

As seen from Table 1, for various processing parameters, the injection pressure necessary to achieve complete wet out changes significantly when a small tapering (α) is introduced on the top and bottom walls of the injection chamber. As tapering of the injection chamber walls increases, the local fiber volume fraction at a given axial location (x) decreases. This lowering of the local fiber volume fraction due to increased CR causes less resistance to the flow of resin; thus, complete wet out is achieved at much lower injection pressures as the taper angle (α) increases.

Figure 4 illustrates the impact of CR on the injection pressure necessary for complete wet out as a function of different pull speeds for both the slot and discrete port injection configurations. For a CR of 1.0 and 1.2, as the pull speed increases, the discrete port injection pressure necessary for complete wet out also increases linearly. The discrete port configuration requires higher injection pressures to achieve complete wet out than the slot injection configuration at $CR = 1.2$. The slope for the discrete port configuration curve at $CR = 1.0$ is higher than that of the discrete port configuration at $CR = 1.2$ and the slot injection configuration at $CR = 1.2$; this indicates that at $CR = 1.0$ the injection pressure rises more rapidly with an increase in pull speed than at $CR = 1.2$ for the slot and discrete port injection configurations. For $CR = 1.2$, the injection pressure necessary to attain complete wet out becomes a weak function of pull speed as the CR increases.

Figure 5 depicts a nonlinear relation between the required discrete port injection pressure for wet out and fiber volume fraction for a CR

Table 1 Injection pressure necessary for complete wet out for different processing parameters for five discrete injection ports of 0.01×0.01 m^2 located 0.1 m from the inlet of the injection chamber

Case No.	CR	Um/s (in./ min)	V_{fo}	μ Pa · s	Injection pressure (gauge) MPa (Psi)
1	1.0	0.015 (36)	0.680	0.75	3.48 (505)
2	1.0	0.020 (48)	0.680	0.75	4.65 (675)
3	1.0	0.025 (60)	0.680	0.75	5.83 (845)
4	1.0	0.025 (60)	0.640	0.75	3.93 (570)
5	1.0	0.025 (60)	0.595	0.75	2.52 (365)
6	1.0	0.025 (60)	0.680	0.50	3.90 (565)
7	1.0	0.025 (60)	0.680	1.00	7.76 (1125)
8	1.2	0.015 (36)	0.680	0.75	0.55 (80)
9	1.2	0.020 (48)	0.680	0.75	0.73 (105)
10	1.2	0.025 (60)	0.680	0.75	0.90 (130)
11	1.2	0.051 (120)	0.680	0.75	1.79 (260)
12	1.2	0.025 (60)	0.595	0.75	0.52 (75)
13	1.2	0.025 (60)	0.640	0.75	0.69 (100)
14	1.2	0.025 (60)	0.724	0.75	1.28 (185)
15	1.2	0.025 (60)	0.680	0.50	0.62 (90)
16	1.2	0.025 (60)	0.680	1.00	1.21 (175)
17	1.2	0.025 (60)	0.680	1.25	1.48 (215)

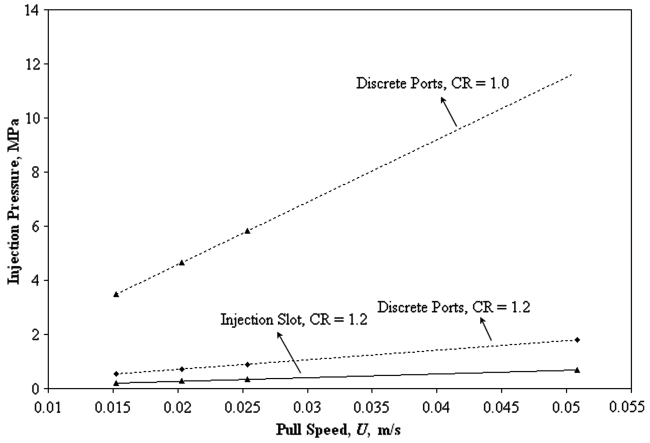

Fig. 4 Injection pressure required for wet out as a function of pull speed for the discrete port configuration at CR = 1.2 ($V_{fo} = 0.68$, $\mu = 0.75$ Pa · s, $H_D = 0.00318$ m, and $W_D = 0.0635$ m).

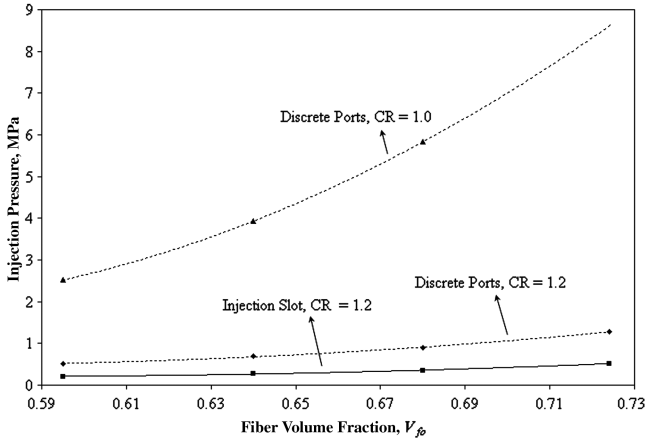

Fig. 5 Injection pressure required for wet out as a function of the fiber volume fraction for the discrete port configuration at CR = 1.2 ($U = 0.0254$ m/s, $\mu = 0.75$ Pa · s, $H_D = 0.00318$ m, and $W_D = 0.0635$ m).

of 1.0 or 1.2. When the final fiber volume fraction (V_{fo}) is increased, the injection pressure required to achieve complete wet out also increases because it becomes more difficult for the resin to penetrate deeper into the fiber reinforcement and reach the center line. For a composite with given fiber volume fraction (V_{fo}), it is observed that, as the CR increases from 1.0 to 1.2, the minimum injection pressure necessary to achieve complete wet out decreases significantly for the discrete port injection configuration because the local fiber volume fraction ($V_f(x)$) decreases as CR increases. Also at CR = 1.2, the discrete port injection configuration requires higher injection pressures than the injection slot configuration to achieve complete wet out. Similarly, Fig. 6 shows the comparison of discrete port injection pressures at CR of 1.0 and 1.2 and the slot injection pressures at CR = 1.2 for various resin viscosities. The curves are linear and the discrete port injection at CR = 1.0 has a much higher slope than the discrete port injection at CR = 1.2 and the injection slot configuration at CR = 1.2. The minimum injection pressure required to achieve complete wet out increases as the resin viscosity increases because a higher viscosity resin offers more flow resistance than a lower viscosity resin. As CR increases, the dependence of injection pressure on the resin viscosity decreases. Figures 4–6 all indicate that, at CR = 1.2, the slot injection configuration yields much lower injection pressures to achieve complete wet out as compared with the discrete injection configuration at a CR of 1.0 and 1.2. Because the slot injection configuration was shown to be preferable to the discrete port injection, further details for the slot injection configuration are shown in the next section.

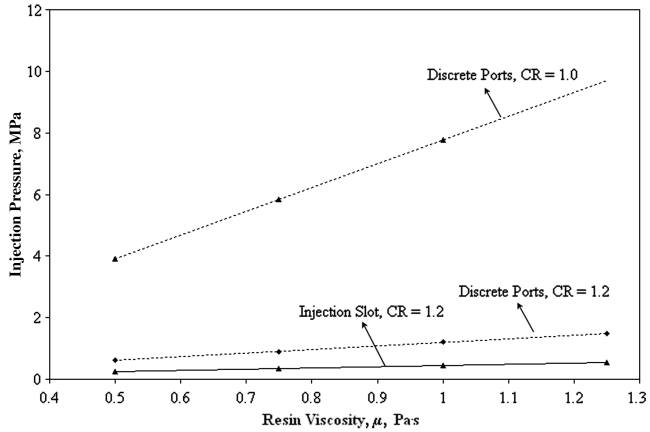

Fig. 6 Injection pressure required for wet out as a function of the resin viscosity for the discrete port configuration at CR = 1.2 ($U = 0.0254$ m/s, $V_{fo} = 0.68$, $H_D = 0.00318$ m, and $W_D = 0.0635$ m).

Slot Injection Configuration

Table 2 lists the minimum injection pressures necessary to achieve complete wet out as a function of the different processing parameters and compression ratios (CR = 1.0, 1.2, 1.5, and 2.0). Complete wet out is not achieved if the injection pressure is below the values reported in Table 2. A small taper (CR > 1) on the walls of the injection chamber and the resin pressure at the exit of the injection chamber have a strong impact on the injection pressure necessary to achieve complete wet out. Table 2 shows that, as the taper angle α increases, the injection pressure required to achieve complete wet out decreases rapidly.

With tapered injection chamber walls (CR > 1.0), the local fiber volume fraction ($V_f(x)$) becomes a monotonically increasing function of the axial coordinate, x. The local fiber volume fraction, $V_f(x)$, is a minimum at the entrance of the injection chamber, increases with increasing axial coordinate, and attains a maximum value at the end of region 1. The local fiber volume fraction at the end of region 1 is the same as the fiber volume fraction of the final composite, that is, $V_f(x) = V_{fo}$; thereafter, the local fiber volume fraction is constant ($V_f(x) = V_{fo}$) through the end of region 2, as region 2 has no taper.

With increasing taper angle (increasing CR), the local fiber volume fraction at a given axial location decreases, hence allowing the liquid resin to penetrate more easily into the fiber matrix by offering less resin flow resistance. Therefore tapering the injection chamber walls helps to achieve complete wet out at lower injection pressures. However, there is a penalty to be paid in that the tapering causes increased injection chamber exit pressures to the level where the die performance may be impaired.

Effect of Pull Speed, U, on the Minimum Injection Pressure Required to Achieve Wet Out with the Slot Injection Configuration

Pull speed is an important process parameter in pultrusion because it impacts productivity; higher pull speeds yield higher cost-effective productivity. Higher pull speeds require higher injection pressures to achieve complete wet out because, as the pull speed increases, the fiber reinforcement more rapidly sweeps the liquid resin downstream and makes it more difficult for the resin to reach the centerline and impregnate the fibers completely.

Cases 18–23, 29–32, 39–42, and 49–52 of Table 2 demonstrate the influence of different pull speeds on the injection pressure required to achieve complete wet out for CR = 1.0, 1.2, 1.5, and 2.0, respectively. The low local fiber volume fraction (at $x = 0.10$ m), $V_f(x)$, due to the taper helps to reduce the injection pressure necessary to achieve complete wet out as the pull speed increases. For a nominal case, $U = 0.0254$ m/s (60 in./min), the injection pressure needed to achieve complete wet out decreases greatly when the walls of the injection chamber are tapered by a small angle of 0.0727 deg (CR = 1.2). For CR = 1.5, the injection pressure is

Table 2 Injection pressure necessary to achieve complete wet out for different processing parameters and compression ratios for an injection slot located 0.1 m from the inlet of the injection chamber

Case No.	CR	Um/s (in./ min)	V_{fo}	μ Pa · s	Injection pressure (gauge) MPa (Psi)
18	1.0	0.0051 (12)	0.680	0.75	0.24 (35)
19	1.0	0.0102 (24)	0.680	0.75	0.45 (65)
20	1.0	0.0150 (36)	0.680	0.75	0.69 (100)
21	1.0	0.0200 (48)	0.680	0.75	0.90 (130)
22	1.0	0.0250 (60)	0.680	0.75	1.14 (165)
23	1.0	0.0510 (120)	0.680	0.75	2.24 (325)
24	1.0	0.0250 (60)	0.595	0.75	0.48 (70)
25	1.0	0.0250 (60)	0.640	0.75	0.72 (105)
26	1.0	0.0250 (60)	0.724	0.75	1.96 (285)
27	1.0	0.0250 (60)	0.680	1.00	1.51 (220)
28	1.0	0.0250 (60)	0.680	0.50	0.75 (110)
29	1.2	0.0150 (36)	0.680	0.75	0.21 (30)
30	1.2	0.0200 (48)	0.680	0.75	0.28 (40)
31	1.2	0.0250 (60)	0.680	0.75	0.35 (50)
32	1.2	0.0510 (120)	0.680	0.75	0.69 (100)
33	1.2	0.0250 (60)	0.595	0.75	0.21 (30)
34	1.2	0.0250 (60)	0.640	0.75	0.28 (40)
35	1.2	0.0250 (60)	0.724	0.75	0.52 (75)
36	1.2	0.0250 (60)	0.680	0.50	0.24 (35)
37	1.2	0.0250 (60)	0.680	1.00	0.45 (65)
38	1.2	0.0250 (60)	0.680	1.25	0.55 (80)
39	1.5	0.015 (36)	0.680	0.75	0.0710 (10)
40	1.5	0.020 (48)	0.680	0.75	0.1050 (15)
41	1.5	0.025 (60)	0.680	0.75	0.1120 (16)
42	1.5	0.051 (120)	0.680	0.75	0.2430 (35)
43	1.5	0.025 (60)	0.595	0.75	0.1050 (15)
44	1.5	0.025 (60)	0.640	0.75	0.1050 (15)
45	1.5	0.025 (60)	0.724	0.75	0.1400 (20)
46	1.5	0.025 (60)	0.680	0.50	0.1050 (15)
47	1.5	0.025 (60)	0.680	1.00	0.1740 (25)
48	1.5	0.025 (60)	0.680	1.25	0.2100 (30)
49	2.0	0.015 (36)	0.680	0.75	0.0021 (0.31)
50	2.0	0.020 (48)	0.680	0.75	0.0021 (0.31)
51	2.0	0.025 (60)	0.680	0.75	0.0021 (0.31)
52	2.0	0.051 (120)	0.680	0.75	0.0021 (0.31)
53	2.0	0.025 (60)	0.595	0.75	0.0160 (2.31)
54	2.0	0.025 (60)	0.640	0.75	0.0090 (1.31)
55	2.0	0.025 (60)	0.724	0.75	0.0021 (0.31)
56	2.0	0.025 (60)	0.680	0.50	0.0021 (0.31)
57	2.0	0.025 (60)	0.680	1.00	0.0021 (0.31)
58	2.0	0.025 (60)	0.680	1.25	0.0021 (0.31)

reduced by about 90% (from 1.14 to 0.112 MPa). Only a small injection pressure (0.0021 MPa, case 51) is needed to achieve complete wet out for CR = 2.0. However, some of these higher CR values may yield an unacceptable resin pressure at the injection chamber exit.

Comparisons of the centerline and die wall pressure profiles along the axial direction for different pull speeds are shown in Fig. 7 for CR = 1.2. Higher pull speeds require a higher injection pressure to achieve complete wet out. Likewise, the resin pressure at the injection chamber exit increases with an increase in the pull speed, as seen in Fig. 7. The energy source for the pressure rise in Fig. 7 comes from the work done by the pultrusion machine, via the puller mechanism (see Fig. 1), in pulling the manufactured composite material through the pultruder. For a CR of 1.2 (see Fig. 7), it is observed that the die wall resin pressure rises to the injection pressure. Next, the die wall resin pressure decreases slightly after the injection slot location and then rises back again. Finally, the die wall resin pressure reaches a maximum at the injection chamber exit. The x location at which the centerline and die wall pressures become equal is the location where complete wet out across the part thickness is achieved. In region 2 ($x > 25$ cm), the pressures are essentially constant (with respect to the x location) because the walls of the injection chamber in region 2 are not tapered.

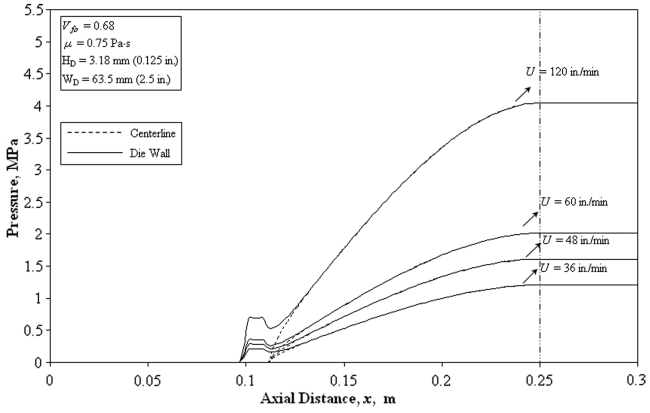

Fig. 7 Centerline and die wall axial pressure (gauge) profiles for CR = 1.2 at different pull speeds for the slot injection configuration.

The isopressure contours and the transient liquid resin flow front development for the nominal processing parameters are shown in Fig. 8 for a CR of 1.2 (case 31). The thick, dark contour corresponds to the liquid resin flow front; the thin lines correspond to the isopressure contours within the liquid resin region. It should be noted that these figures are "not to scale"; this was done to make the results more "viewable" and understandable. The actual composite in Fig. 8 corresponds to a very long and very thin domain, which makes it useful for displaying the results geometrically not to scale. The liquid resin is seen to be swept downstream and to flow toward the centerline as time progresses.

Figure 9 illustrates the impact of the tapering of the injection chamber walls (CR) on the injection pressure required to attain complete wet out and the resin pressure at the exit of the injection

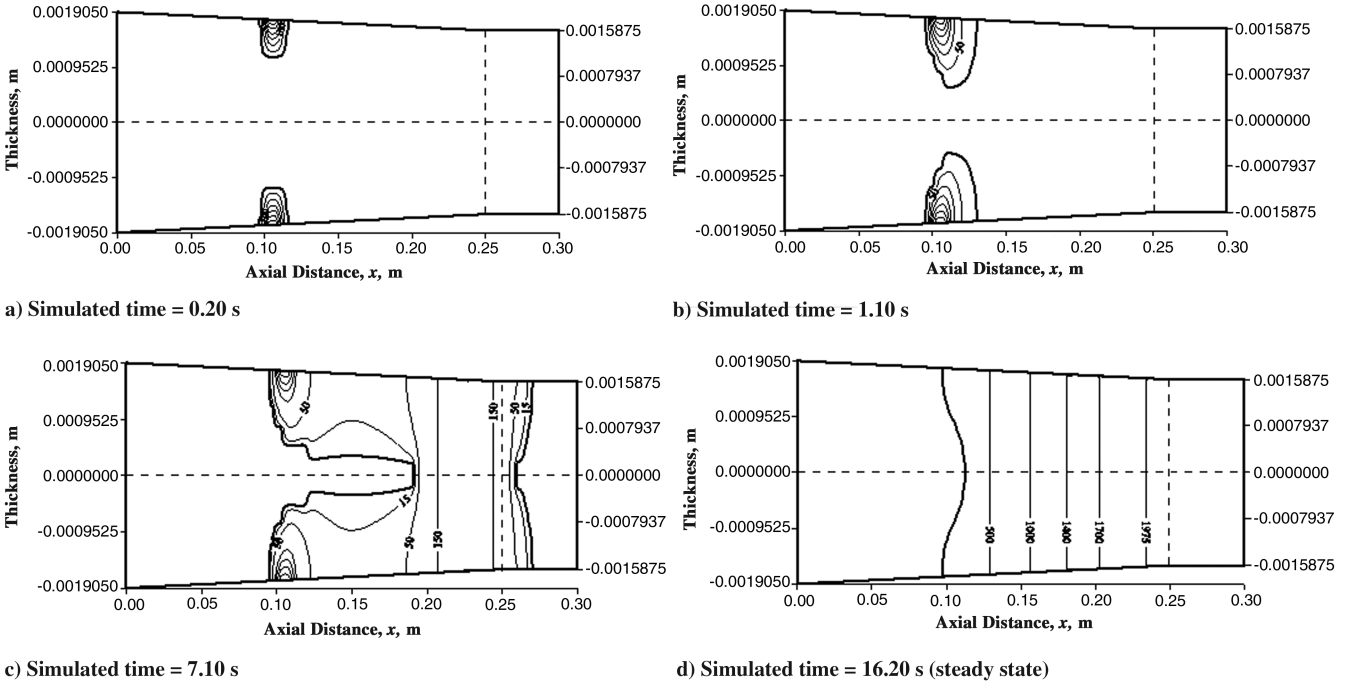

Fig. 8 Transient flow front profile and gauge isopressure (kPa) contours for the polyester resin/glass roving composite and slot injection configuration, CR = 1.2, $U = 0.0254$ m/s, $V_{fo} = 0.68$, $\mu = 0.75$ Pa · s, and slot location = 0.1 m (case 31) (not to scale).

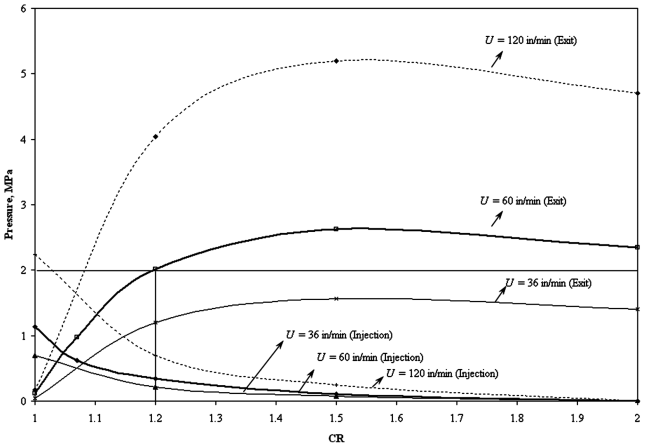

Fig. 9 Injection and exit pressures as a function of CR for different pull speeds ($V_{fo} = 0.68$, $\mu = 0.75$ Pa · s, and slot location = 0.1 m).

chamber for different pull speeds ($U = 0.0152$, 0.0254, and 0.0508 m/s). As seen in Fig. 9, when CR increases, the injection pressure required to achieve complete wet out decreases and the resin pressure at the injection chamber exit increases; the exit pressure increases rapidly as CR increases and does not change much after CR = 1.3. For pull speeds of 0.015 and 0.0508 m/s, the injection pressure and the exit resin pressure become equal at about CR = 1.07; below CR = 1.07, the injection pressure is higher and, beyond CR = 1.07, the exit resin pressure is higher than the injection pressure. Similarly, for a pull speed of 0.0254 m/s, the injection and exit pressures become equal at about CR = 1.05; the injection pressure is higher when CR is less than 1.05, and the exit pressure is greater than the injection pressure if CR is more than 1.05.

The curves in Fig. 9 provide useful information for the injection chamber and the pultrusion die designer. For a given pull speed, the maximum pressure that the injection chamber and the pultrusion die can handle is first selected with safety and design considerations in mind (ordinate of Fig. 9). A horizontal line is drawn for the selected maximum design pressure. Next, a vertical line is drawn from the point at which the horizontal line intersects the exit pressure curve; the point at which the vertical line intersects the injection pressure curve yields the injection pressure necessary to achieve complete wet out, and the point at which this vertical line intersects the horizontal axis is the CR value to be selected according to the given design constraints. A reasonable value of exit resin pressure is desirable because it helps to suppress voids in the resin and fiber matrix. For example, using Fig. 9 modeled for different pull speeds, selecting an exit pressure of around 1 MPa (145 psi) with $U = 0.254$ m/s shows that an injection pressure of approximately 0.6 MPa (87 psi) injected about 0.10 m into an injection chamber with CR = 1.07 is required for complete wet out. If the pultrusion die/injection chamber design could support a 2-MPa (∼300-psi) internal resin pressure, then only 0.3 MPa (43 psi) of injection pressure would be required using an injection slot located 0.10 m into an injection chamber with CR = 1.2.

Effect of Fiber Volume Fraction, V_{fo}, on Minimum Injection Pressure Required to Achieve Wet Out for the Slot Configuration

The fiber volume fraction (V_{fo}) determines the strength of the final composite. Typically, higher fiber volume fraction composites have higher strength. Composites having final product fiber volume fractions (V_{fo}) of 0.595, 0.640, 0.680, and 0.724 were simulated, with $V_{fo} = 0.680$ as the nominal value.

Cases 22, 24, 25, 26, 31, 33, 34, 35, 41, 43, 44, 45, 51, 53, 54, and 55 of Table 2 depict the slot injection pressures required to achieve wet out for a CR of 1.0, 1.2, 1.5, and 2.0, respectively, at different V_{fo}. For CR = 1.0, 1.2, and 1.5, it is seen that, as the fiber volume fraction increases, higher injection pressures are needed to achieve complete wet out because a fiber matrix with high fiber volume fractions offer more resistance to the flow of resin through the fiber reinforcement. For CR = 2.0, only a low injection pressure (0.0021 MPa, gauge) is required to achieve complete wet out, and the minimum injection pressure to achieve complete wet out is essentially a weak function of the fiber volume fraction.

The centerline and die wall pressure profiles for different fiber volume fractions are illustrated in Fig. 10 for a CR of 1.2; a composite with a high fiber volume fraction requires a higher injection pressure to achieve complete wet out. In addition, the resin pressure at the exit of the injection chamber likewise increases with an increase in the fiber volume fraction, as seen in Fig. 10.

Figure 11 demonstrates the impact of the tapering of the injection chamber walls (CR) on the injection pressure required to attain

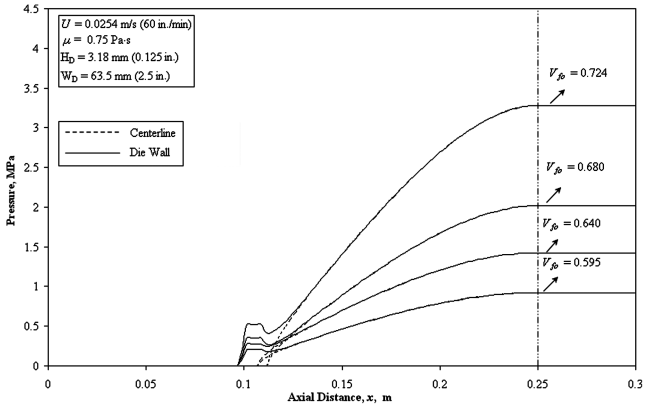

Fig. 10 Centerline and die wall axial pressure (gauge) profiles for CR = 1.2 at different fiber volume fractions for the slot injection configuration.

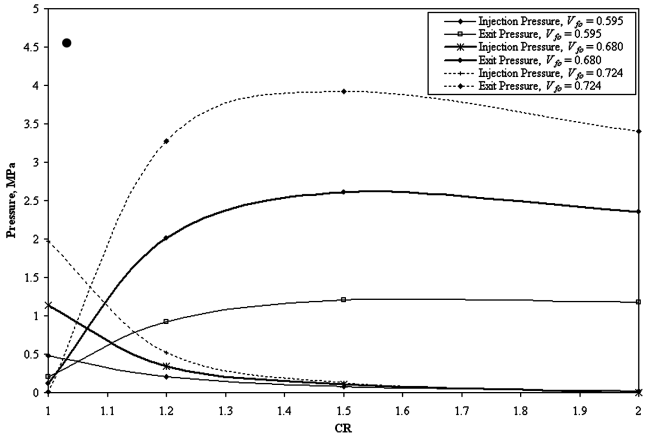

Fig. 11 Injection and exit pressures as a function of CR for different fiber volume fractions ($U = 0.0254$ m/s, $V_{fo} = 0.68$, $\mu = 0.75$ Pa · s, and slot location = 0.1 m).

complete wet out and the resin pressure at the exit of the injection chamber for different fiber volume fraction composites ($V_{fo} = 0.595$, 0.680, and 0.724). The injection pressure required to achieve complete wet out decreases and the resin pressure at the injection chamber exit increases as CR increases; beyond CR = 1.3, the exit pressure does not change much as compared with below CR = 1.3 (see Fig. 11). The injection pressure and the exit resin pressure become equal at about CR = 1.07 for composites with 0.680 and 0.724 fiber volume fractions. Similarly, for a composite with a 0.595 fiber volume fraction, the injection and exit pressures become equal at about CR = 1.05; the injection pressure is higher than the exit resin pressure when CR is less than 1.05, and the exit pressure is greater than the injection pressure if CR is more than 1.05. The curves in Fig. 11 provide useful design information for the injection chamber and the pultrusion die when the fiber volume fraction is varied. For a composite with given fiber volume fraction, the maximum pressure the injection chamber and the pultrusion die can handle is selected (ordinate of Fig. 11) from safety and design considerations. A horizontal line is drawn for the corresponding selected maximum design pressure. When the fiber volume fraction in a composite is to be varied, for design purposes, Fig. 11 can be used in a similar manner as that explained for Fig. 9.

Effect of Resin Viscosity, μ, on the Minimum Injection Pressure Required to Achieve Complete Wet Out for the Slot Configuration

The initial resin viscosity depends on factors such as the type of resin and amount of filler. Curing of the resin before the complete wet out of the fiber reinforcement is achieved is not desirable, and so it is assumed that the resin viscosity is held constant as isothermal conditions prevail throughout the resin injection chamber. High

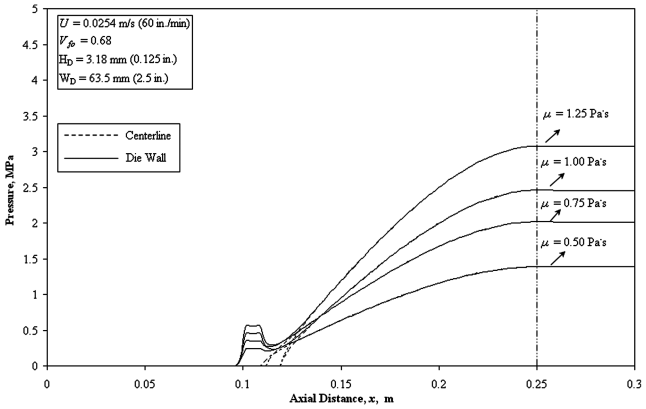

Fig. 12 Centerline and die wall axial pressure (gauge) profiles for CR = 1.2 at different resin viscosities for the slot injection configuration.

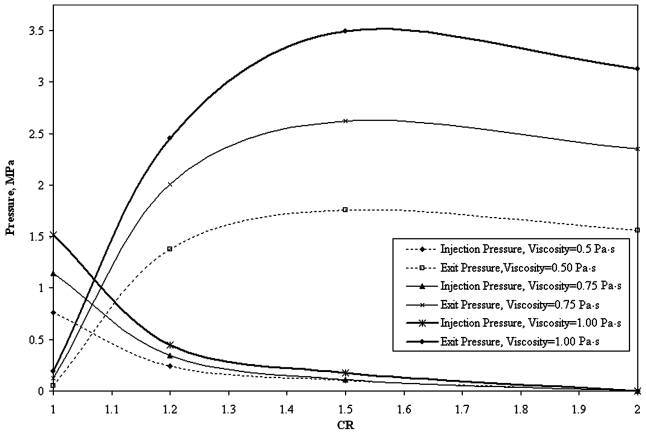

Fig. 13 Injection and exit pressures as a function of CR for different resin viscosities ($U = 0.0254$ m/s, $V_{fo} = 0.68$, and slot location= 0.1 m).

viscosity resins require high injection pressures to achieve wet out as they offer more resistance to flow through the fiber matrix; a low viscosity requires less injection pressure to achieve complete wet out. The predicted injection pressure necessary for complete wet out for a polyester resin with $\mu = 0.50$, 0.75, 1.00, and 1.25 Pa · s viscosities is summarized in Table 2 for a CR of 1.0, 1.2, 1.5, and 2.0, respectively (cases 22, 27, 28, 31, 36, 37, 38, 41, 46, 47, 48, 51, 56, 57, and 58).

Figure 12 illustrates the centerline and die wall pressure profiles for different resin viscosities and CR = 1.2 for the slot injection configuration. As the resin viscosity increases, the injection pressure required to achieve complete wet out and the resin pressure at the exit of the injection chamber are likewise seen to increase. The location at which the die wall and centerline pressures become equal (meet) is the axial location at which the resin reaches the centerline and wet out is complete. Figure 13 depicts the impact of the CR value on the injection pressure required to achieve complete wet out and the corresponding resin exit pressure. The injection pressure decreases and the resin pressure at the injection chamber exit increases as CR increases. The injection pressure and the exit resin pressure become equal at about CR = 1.07 for different resin viscosities ($\mu = 0.50$, 0.75, and 1.00 Pa · s). Figure 13 provides useful design information for the injection chamber and the pultrusion die when the resin viscosity is varied and the fiber volume fraction and pull speed are held constant. Again, it is seen that, for moderate injection pressures and moderate exit pressures, a CR value of about 1.07 is a good choice.

Conclusions

The numerical model developed is a useful and important tool to predict the impact of various process control parameters related to the

pultrusion manufacturing of polymeric composites and to understand their effect on the wet out, the injection pressure necessary to achieve complete wet out, and the location of the liquid resin flow front. The simulation results from the numerical technique can be used to select the value of tapering (Figs. 9, 11, and 13) that would result in moderate injection and exit resin pressures. The numerical model is a useful guide to the experimental work as it identifies the sensitivity and range of the processing parameters. It has been shown that, for the high pull speed resin injection pultrusion manufacturing of a polyester/glass roving composite, the slot injection configuration is favorable to the discrete port injection configuration. Lower injection pressures are needed for the slot injection configuration to achieve complete wet out as opposed to the discrete port configuration. The simulation results predicted a linear increase in the injection pressure necessary for complete wet out as a function of pull speed or resin viscosity. A nonlinear behavior in the injection pressure for complete wet out was observed with an increase in the fiber volume fraction of the composite (for $CR < 1.2$). It has been shown that a compression ratio of about $CR = 1.07$ is desirable to achieve complete wet out at both moderate injection and chamber exit pressures.

Acknowledgments

The authors want to thank Ellen Lackey and James Vaughan for their valuable insight and recommendations during the course of this work.

References

[1] Lackey, E., Vaughan, J. G., and Roux, J. A., "Experimental Development and Evaluation of a Resin Injection System for Pultrusion," *Journal of Advanced Materials / Society for the Advancement of Material and Process Engineering*, Vol. 29, Oct. 1997, pp. 30–37.

[2] Dube, M. G., Batch, G. L., Vogel, H. H., and Macosko, C. W., "Reaction Injection Pultrusion of Thermoplastic and Thermoset Composites," *Polymer Composites*, Vol. 16, No. 5, 1995, pp. 378–385. doi:10.1002/pc.750160506

[3] Kim, Y. R., "Behavior of Fiber Reinforcement and Resin Flow During the Injection Pultrusion Process," Ph.D. Thesis, University of Massachusetts, Lowell, MA, 1990.

[4] Lee, I. J., Young, W. B., and Lin, R. J., "Mold Filling and Cure Modeling of RTM and SRIM Processes," *Composite Structures*, Vol. 27, Nos. 1–2, 1993, pp. 109–20.

[5] Bruschke, M. V., and Advani, S. G., "A Finite Element/Control Volume Approach to Mold Filling in Anisotropic Porous Media," *Polymer Composites*, Vol. 11, No. 6, 1990, pp. 398–405. doi:10.1002/pc.750110613

[6] Varma, R. R., and Advani, S. G., "Three-Dimensional Simulations of Filling in Resin Transfer Molding," *Advances in Finite Element Analysis in Fluid Dynamics*, Vol. 200, American Society of Mechanical Engineers, Fluids Engineering Division, New York, 1994, pp. 21–27.

[7] Trochu, F., Boudreault, J. F., Gao, D. M., and Gauvin, R., "Three Dimensional Flow Simulation for the Resin Transfer Molding Process," *Materials and Manufacturing Processes*, Vol. 10, No. 1, Jan. 1995, pp. 21–6. doi:10.1080/10426919508934995

[8] Liu, X. L., "A Finite Element/Nodal Volume Technique for Flow Simulation of Injection Pultrusion," *Composites. Part A, Applied Science and Manufacturing*, Vol. 34, No. 7, July 2003, pp. 649–661. doi:10.1016/S1359-835X(03)00085-X

[9] Liu, X. L., "Iterative and Transient Numerical Models for Flow Simulation of Injection Pultrusion," *Composite Structures*, Vol. 66, Nos. 1–4, Oct.–Dec. 2004, pp. 175–180. doi:10.1016/j.compstruct.2004.04.035

[10] Ding, Z., Li, S., Yang, H., and Lee, L. J., "Numerical and Experimental Analysis of Resin Flow and Cure in Resin Injection Pultrusion (RIP)," *Polymer Composites*, Vol. 21, No. 5, 2000, pp. 762–778. doi:10.1002/pc.10231

[11] Ding, Z., Li, S., and Lee, L. J., "Influence of Heat Transfer and Curing on the Quality of Pultruded Composites 2: Modeling and Simulation," *Polymer Composites*, Vol. 23, No. 5, 2002, pp. 957–969. doi:10.1002/pc.10493

[12] Rahatekar, S. S., and Roux, J. A., "Numerical Simulation of Pressure Variation and Resin Flow in Injection Pultrusion," *Journal of Composite Materials*, Vol. 37, No. 12, 2003, pp. 1067–1082. doi:10.1177/0021998303037012005

[13] Kommu, S., Khomami, B., and Kardos, J. L., "Modeling of Injection Pultrusion Processes: A Numerical Approach," *Polymer Composites*, Vol. 19, No. 4, 1998, pp. 335–346. doi:10.1002/pc.10106

[14] Voorakaranam, S., Joseph, B., and Kardos, J. L., "Modeling and Control of an Injection Pultrusion Process," *Journal of Composite Materials*, Vol. 33, No. 13, 1999, pp. 1173–1202.

[15] Raper, K. S., Roux, J. A., Vaughan, J. G., and Lackey, E., "Permeability Impact on the Pressure Rise in a Pultrusion Die," *Journal of Thermophysics and Heat Transfer*, Vol. 13, No. 1, Jan.–March 1999, pp. 91–99.

[16] Patankar, S., *Numerical Heat and Fluid Flow*, Hemisphere, New York, 1980.

[17] Darcy, H., *Les Fontaines Publique de la Ville de Dijon*, Dalmont, Paris, 1856.

[18] Raper, K. S., Roux, J. A., McCarty, T. A., and Vaughan, J. G., "Die Inlet Contour Impact on the Pressure Rise in a Pultrusion Die," *Journal of Composite Materials*, Vol. 34, No. 3, Feb. 2000, pp. 199–217. doi:10.1106/EDTV-6YGD-0JTX-9KV4

[19] Gutowski, T. G., Cai, A., Bauer, S., Boucher, D., Kingery, J., and Wineman, S., "Consolidation Experiments for Laminate Composites," *Journal of Composite Materials*, Vol. 21, No. 7, July 1987, pp. 650–669. doi:10.1177/002199838702100705